How important are aerosol–fog interactions for the successful modelling of nocturnal radiation fog?

C. Poku,[1] A. N. Ross,[1] A. M. Blyth,[1,2] A. A. Hill,[3] and J. D. Price[3,4]

[1]*School of Earth and Environment, University of Leeds*
[2]*National Centre for Atmospheric Science, University of Leeds*
[3]*Met Office, Exeter*
[4]*Met Office Research Unit, Cardington Airfield, Shortstown*

Introduction

Fog, which can be defined as a cloud at ground level with surface visibility less than 1km, can cause major disruption to road, aviation and marine transport, with associated economic losses that are comparable to those resulting from winter storms and hurricanes (Gultepe *et al.*, 2007). Fog can also have negative impacts on human health and the safety of certain activities. For example, thick fog on 5 September 2013 resulted in the Sheppey crossing crash in southeast England, which involved 130 vehicles and resulted in injuries to 60 people (BBC, 2013). Understanding the physics behind fog is crucial in improving fog forecasting and mitigating the impact of such fog events. Whilst there are several different types of fog (Tardif *et al.*, 2007), the two types most commonly experienced in the United Kingdom are radiation and advection fog. What both of these have in common is that they depend on a number of small-scale physical processes (radiative, turbulent, thermodynamical, microphysical) which result in an air mass becoming saturated (relative humidity equal to 100%) with the consequent formation of fog. This study focuses on the influence of aerosols on the formation of nocturnal radiation fog.

Aerosols are small particles suspended in the atmosphere, with a range of sizes and compositions (Pruppacher and Klett, 2010). Aerosols are important for fog, as they act as the substrate on which water condenses and fog droplets form. The droplet growth rate is dependent on the initial aerosol size and their solubility. The aerosols are considered to be 'activated' once these droplets reach a certain size, where they can grow more easily within a saturated environment. Aerosols that can act as a substrate for droplets are known as cloud condensation nuclei (CCN). Microphysical properties and aerosol–fog interactions are critical in determining the formation and resulting evolution of the fog (see Figure 1). At night, prior to fog forming, the ground and lower layers of the atmosphere will experience radiative cooling. The rate of cooling is influenced by the synoptic conditions: high-pressure systems with low wind speeds and reduced cloud cover can result in a cooling rate sufficient for fog formation (Price, 2011). As the lower layers of the atmosphere cool, the relative humidity increases and water vapour will condense onto CCN to form fog droplets and a thin fog layer. The number of activated aerosols (fog droplets) depends on the aerosol size distribution and concentration, as well as the rate of cooling at the surface. The fog layer will absorb and emit longwave radiation, and as the layer thickens, longwave cooling will be strongest at the fog top. The result is that the fog layer becomes well-mixed (with a constant temperature profile within the layer) through convection, increasing its optical thickness. However, the turbulence levels and the humidity profile during fog formation can result in the fog remaining optically thin (Price *et al.*, 2018).

Although research into radiation fog spans the last 100 years (e.g. Taylor, 1917; Roach *et al.*, 1976), the greater recognition of the role of aerosols has been studied only in recent decades. Bott (1991) discussed the importance of aerosol–fog interactions, where they fundamentally control the optical thickness of nocturnal fog. Additional studies have complemented the work by Bott (e.g. Stolaki *et al.*, 2015; Maalick *et al.*, 2016). More recently, Boutle *et al.* (2018) demonstrated the importance of aerosol–fog interactions in Numerical Weather Prediction (NWP) and, in particular, cases of fog that may form within a relatively clean environment.

This study aims to understand the role of aerosol–fog interactions on the evolution of a nocturnal optically thin fog layer, by performing and comparing various high-resolution numerical simulations with different aerosol properties. Simulations are undertaken with the Met Office and Natural Environment Research Council Cloud (MONC) model (Brown *et al.*, 2015; 2018), which is a newly developed large eddy simulation model that is a complete rewrite of the Met Office Large Eddy Model (Gray *et al.*, 2001). MONC is an atmospheric

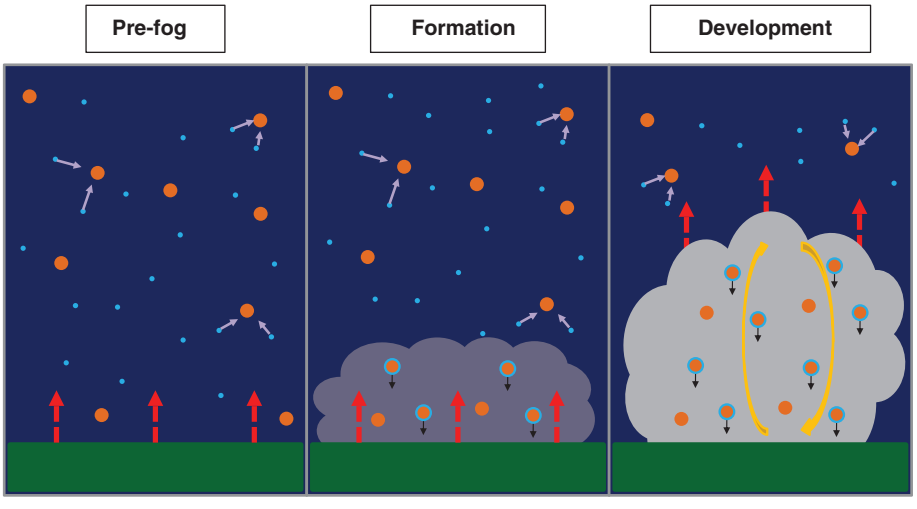

Figure 1. Schematic demonstrating the three stages of the evolution of nocturnal radiation fog: pre-fog, fog formation and fog development. Orange dots – CCN; light blue dots – water vapour; red arrows – radiative cooling; yellow arrows – convection; black arrows – sedimentation by gravity.

process model designed for research and development of parameterisations for the forecast model. For this work, MONC has been coupled up with the Cloud AeroSol Interactive Microphysics (CASIM) scheme, which has been developed at the Met Office as a long-term replacement for the Met Office Unified Model (MetUM) microphysics scheme. CASIM has been specifically developed to simulate and investigate aerosol–cloud interactions in the MetUM (e.g. Field *et al.*, 2016; Grosvenor *et al.*, 2017; Miltenberger *et al.*, 2018; Stevens *et al.*, 2018) and MONC (Dearden *et al.*, 2018). This study attempts to address two key objectives:

1. Evaluate how well MONC coupled with the CASIM scheme can simulate an optically thin nocturnal fog case;
2. Investigate the influence of aerosol properties on fog development.

Whilst there are other processes that are important for the fog life cycle, such as surface interactions, they are outside the scope of this study.

Model setup

MONC is used to perform a suite of sensitivity tests based on IOP1 (intensive observation period 1) from the recent Local And Non-local Fog EXperiment (LANFEX) field campaign (Price *et al.*, 2018). IOP1 took place at the UK Met Office research field site at Cardington, Bedfordshire in south-east England (52°06'N, 0°25.5'W) on 24/25 November 2014. The site sits in a wide, shallow valley characterised by a patchwork of mostly arable fields with low hedges. During the night of IOP1 a high-pressure system had developed across most of the UK, resulting in widespread fog. At Cardington, fog formed around 1800 UTC and remained stable, as well as optically thin, through the duration of the night. IOP1 was chosen as it was one of the cleanest examples of local fog development, with minimal influence by advective processes (see Smith *et al.*, 2018 for more details).

Table 1

Input parameters and model set up for IOP1 in MONC.

IOP 1	
Horizontal domain	132 × 132m
Vertical domain	705m
Δx, Δy	2m
Δz	Variable – 1m first 100m, stretched up to 6m afterwards
Simulation duration	12h
Timestep	0.1s
Cloud microphysics	Cloud AeroSol Interactive Microphysics (CASIM)
Radiative transfer scheme	SOCRATES (Edwards and Slingo, 1996)

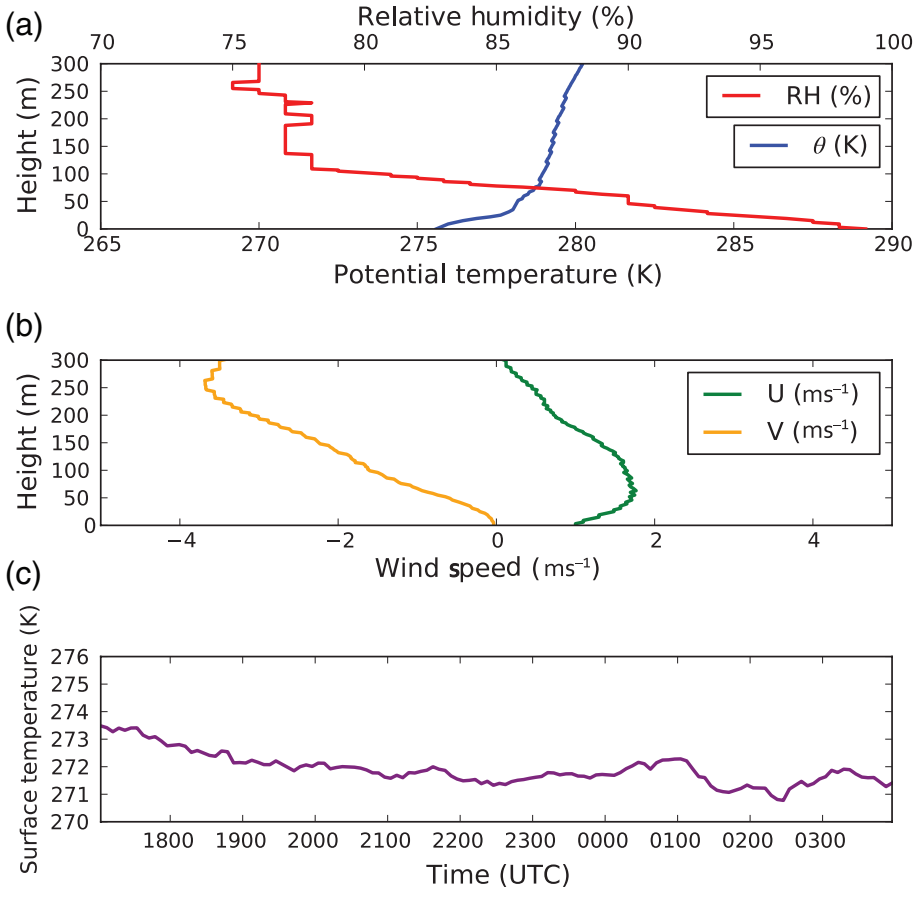

Figure 2. Initial conditions at 1700 UTC used to initialise MONC. From radiosonde data: (a) potential temperature (K) and relative humidity (%) and (b) wind components. From surface measurements: (c) grass surface infrared-derived temperature.

The model setup for IOP1 is presented in Table 1. MONC was initialised using the observed vertical profiles and surface measurements as shown in Figure 2. The grid spacing in MONC was 2 × 2m in the horizontal and 1m in the vertical up to 100m. Previous studies have shown the importance of model resolution for simulating the formation period of fog (e.g. Maalick *et al.*, 2016; Maronga and Bosveld, 2017); it was therefore critical to run MONC at such a high resolution. A surface temperature as shown in Figure 2(c) and a surface vapour mixing ratio of 0.004kgkg^{-1} were both prescribed based on observations. Thus, these simulations do not include an interactive land surface. While surface atmosphere interactions and feedbacks can be very important for fog, observed surface fluxes from IOP1 were close to zero or negative (not shown), so feedbacks between the surface and atmosphere may not be as important for IOP1 compared with other fog cases (Boutle *et al.*, 2018). Radiation was calculated using the Suite of Community RAdiative Transfer codes (SOCRATES), based on the work of Edwards and Slingo (1996). SOCRATES was called by the MONC model every 5min, allowing for the longwave radiative fluxes at the top of the fog layer to be captured in the model. The longwave radiative fluxes are determined by the cloud's optical depth, τ, (which is dependent on the cloud's effective radius, r_e), and the weighted mean droplet size for a given population of cloud droplets (Edwards and Slingo, 1996). Throughout this study, MONC coupled with SOCRATES assumes a fixed effective radius, such that r_e = 10μm. The chosen radius is the default value for MONC and is primarily motivated by observations of the effective radius within cumulus clouds (Blyth and Latham, 1991). Although this value may not be suitable for simulations of fog, investigating the effective radius was outside the scope of this work.

All simulations use CASIM, as described above. In this work, CASIM is configured to use two moments (mass and number

concentration of cloud and rain), as well as mass and number concentration of multi-mode aerosols (aerosols of different sizes). For the aerosol population, only large CCN (those in the accumulation mode where 0.1μm < CCN size diameter < 1μm) are accounted for, and its size distribution is assumed to be lognormal with a standard deviation of 2.0. The aerosol activation scheme used in these simulations is that of Abdul-Razzak and Ghan (2000), which uses an average CCN size that is determined by the total soluble mass, the CCN number concentration and an assumed aerosol size distribution. In-cloud processing of aerosol removal is turned off in these simulations for consistency with previous studies (e.g. Stolaki *et al.*, 2015; Maalick *et al.*, 2016).

Table 2 summarises the setup of the simulations presented in this study. There were five simulations run (as listed in the Table 2) – these are described in the following sections. During IOP1, there were no direct observations of CCN. A value of 100cm^{-3} in the accumulation mode was set, with a total soluble mass of 2.7ng throughout the initialised vertical profile, based on typical measurements for a clean rural site similar to Cardington, UK (Boutle *et al.*, 2018). To reduce computational expense, 1D diagnostics are output every 1min and 3D diagnostics are output every 5min.

Control simulation – T_control

This section describes the control simulation, T_control, which will be directly compared with observations from IOP1 and will form the basis for further sensitivity tests. Observations show (Figure 3) the visibility at a 2m height dropping below 1000m at around 1800 UTC, and then decreasing further to 100m at 2100 UTC. After 2100 UTC the fog remained optically thin, with visibility varying between 1000m and 100m, implying that the fog was patchy throughout the night.

For all model simulations, the visibility is calculated using the formula of Gultepe *et al.* (2006), where visibility, *Vis*, is defined as follows:

$$Vis = \frac{1.002}{(LWC \times CDNC)^{0.6473}} \quad (1)$$

where *LWC* is the liquid water content and CDNC is the cloud droplet number concentration. Equation 1 was derived based on observations of fog in mainland Europe and is valid over a range of CDNC from a few per cubic centimetre up to a few hundred per cubic centimetre. The simulated visibility at a 2m height in T_control drops under 1km at 1700 UTC, indicating the formation of fog an hour prior to observations, where it continues to decrease and eventually converges to around 160m. The small visibility range before 2245 UTC, demonstrated by the difference between the minimum and maximum, shows a spatially homogeneous layer of fog. However, after 2245 UTC the range increases, showing a more heterogeneous layer, which is indicative of a more turbulent boundary layer. The variability in the simulated visibility across the domain is similar to the temporal variability in the observed visibility for parts of the night, particularly later on. However, the visibility in T_control within the initial stages is mostly lower than the observations, implying that T_control is producing optically thick fog too quickly. Consistent with this, a mixed layer develops much earlier in the simulated boundary layer than in observations (not shown).

Vertical profiles of CDNC were taken throughout the night, as shown in Figure 4. At 2230 UTC, the highest concentration of fog droplets is within the lowest 10m, at around 100cm^{-3}. The CDNC gradually decreases with height, and from 20m it increases again to a maximum of 50cm^{-3} at a height of 37m. The CDNC indicates the height of the fog, which at 2230 UTC is 50m. At 0030 UTC, the peak concentration of fog droplets occurs at the top of the fog: 100cm^{-3} at a height of 40m. Although it appears as though the fog layer has decreased in height, one possible explanation for the decrease in the observed CDNC could be an instrumentation error which resulted in only cloud droplets that were of sizes between 2 and 50μm in diameter being accounted for, with a 1μm uncertainty (Price *et al.*, 2018). Finally, at 0330 UTC there is a greater variation in CDNC, although it is beginning to homogenise in the middle part of the layer, and it ranges between 20 and 100cm^{-3}. The peak CDNC is at 40m, and the fog layer depth is 65m.

Throughout the night, the activation rate in T_control (the percentage of CCN that activates into fog droplets), is between 60 and 70%. At 2230 UTC, whilst the difference in fog layer height between T_control and the observations is only 4m, the proportion of fog droplets averaged over the depth of the fog in T_control is greater than the observations by a factor of 2.1 (Table 3). Following

Table 2

List of tests referred to throughout this study, which includes changes in aerosol properties.

Test	*CCN concentration (cm^{-3})*	*Total soluble mass (ng)*	*Average CCN radius (μm)*
T_control	100	2.7	0.075
T_double_ccn	200	2.7	0.059
T_half_ccn	50	2.7	0.094
T_double_mass	100	5.4	0.094
T_half_mass	100	1.35	0.059

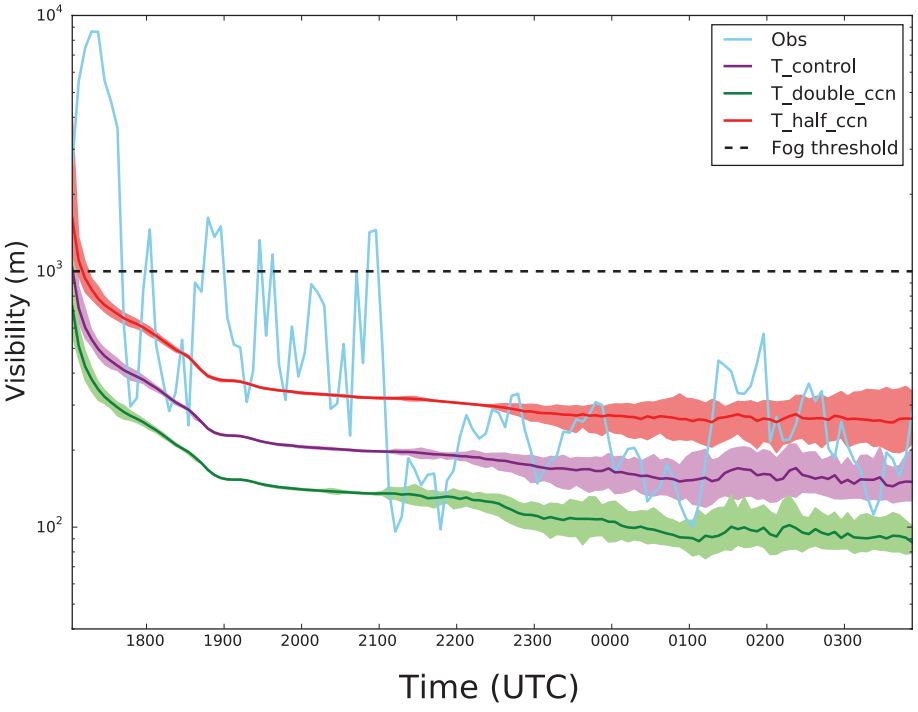

Figure 3. Time series of mean visibility (m) at 2m height. Purple: T_control; green: T_double_ccn; red: T_half_ccn; light blue: observations. The shaded areas of each colour denote the maximum and minimum visibility of each simulation.

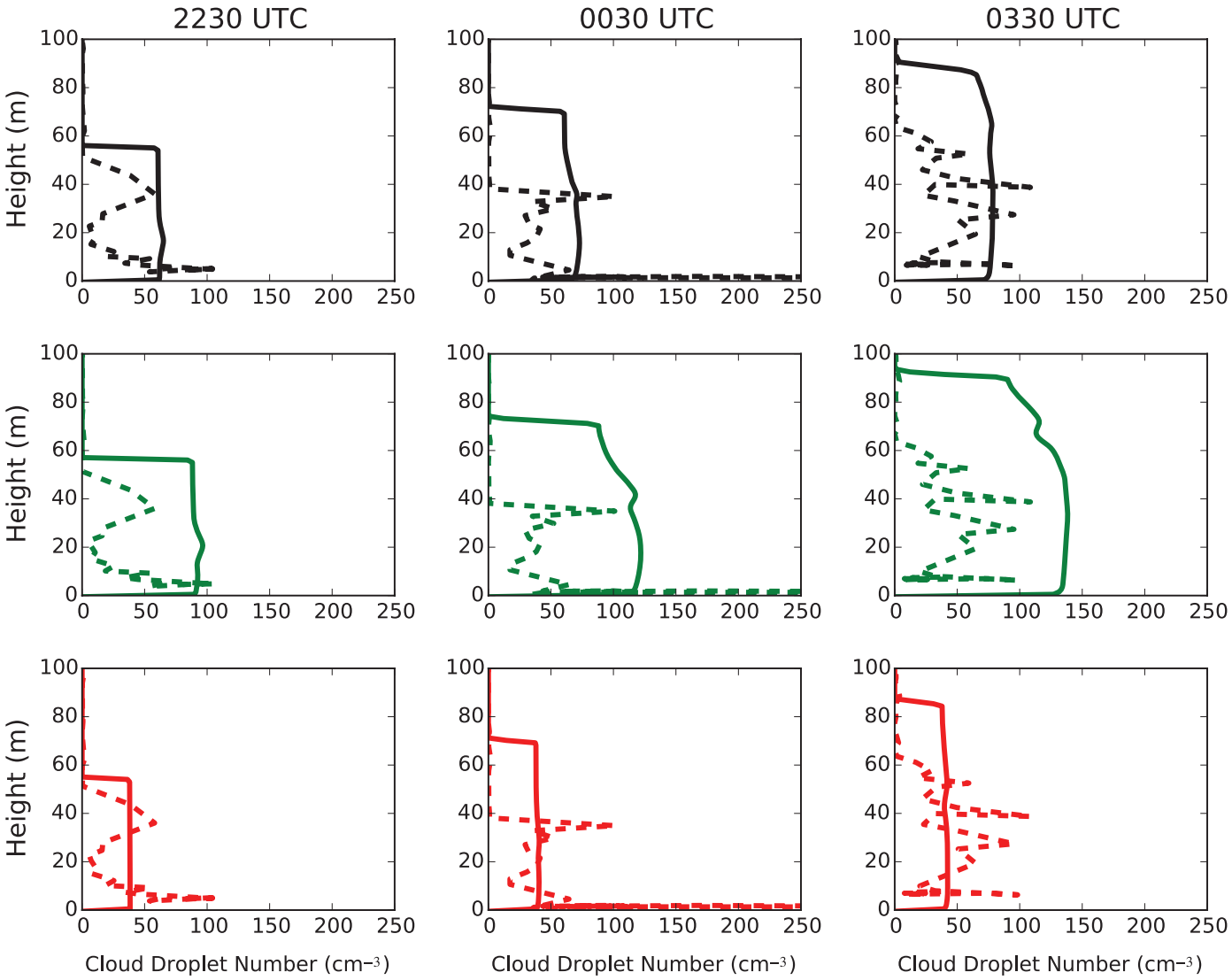

Figure 4. Vertical profiles of cloud droplet number concentration (cm^{-3}) at 2230, 0030 and 0330 UTC. The dashed lines represent observations, and solid lines represent simulated values. Black: T_control; green: T_double_ccn; red: T_half_ccn.

Table 3

Table listing the ratio of modelled to observed cloud drop number averaged over the vertical height across tested time frames.

Test	*Time (UTC)*		
	2230	*0030*	*0330*
T_control	2.1	1.2	2.5
T_double_ccn	3.2	1.9	4.1
T_half_ccn	1.3	0.7	1.4
T_double_mass	2.3	1.2	2.5
T_half_mass	1.9	1.1	2.2

on, at 0030 UTC the height of the fog layer in T_control is greater than the observations by 30m, with T_control forming an average of 1.2 times as many fog droplets across the fog depth. Finally, at 0330 UTC the fog layer has a greater height by 30m in T_control in comparison to observations, with an average of 3.5 times more fog droplets across the fog depth. The number of droplets formed is determined by the aerosol activation parameterisation. The majority of activation schemes (including the scheme in CASIM) were designed for convective cloud formation (Ghan *et al.*, 2011). Discrepancies within the scheme may be the main cause of too many droplets forming within T_control. These discrepancies will be discussed in more detail in a moment.

Observations show a general increase in the liquid water path (LWP, the integrated liquid water across the vertical depth) throughout the time period (Figure 5), with a maximum mean LWP of $15 gm^{-2}$ (calculated using a 40-point running average) at around 0330 UTC. The maximum mean LWP occurred around the same time that the visibility at 2m dropped below 100m, as shown in Figure 3, suggesting that this was a key stage at which the fog became optically thicker. Throughout the T_control simulation, the modelled mean LWP mostly agreed with the observed averaged LWP, although it was on the lower range of the variability up until 0100 UTC. Work by Stolaki *et al.* (2015) demonstrated how the LWP is controlled by the rate of sedimentation, with Boutle *et al.* (2018) showing that the LWP is controlled by both the LWC and the cloud droplet number concentration. Therefore, this result suggests that the fog produced by T_control becoming optically thick too quickly is primarily due to the presence of too many droplets, which could link back to the representation of aerosol activation.

CCN sensitivity tests

Previous studies (e.g. Bott, 1991; Stolaki *et al.*, 2015; Maalick *et al.*, 2016) show how features of the evolution of fog, in particular the fog optical depth, are influenced by CCN properties. We will now investigate how the CCN number concentration and size could influence the transition to optically thick fog. To address this, two additional simulations were conducted. The first set involved fixing the total soluble mass used in T_control whilst doubling and halving the CCN

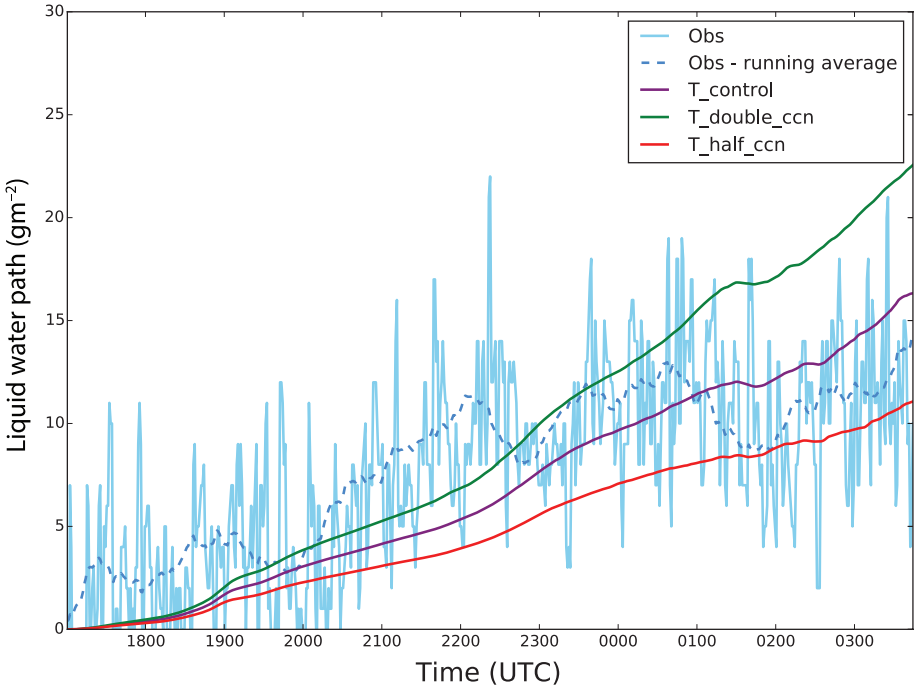

Figure 5. Time series of liquid water path (gm^{-2}). Purple – T_control; green – T_double_ccn; red – T_half_ccn; sky blue – observations; blue dashed – running average over observations (40 points).

concentration to 200 and 50cm^{-3} respectively (referred to as tests T_double_ccn and T_half_ccn). The second set involved fixing the CCN number concentration used in T_control whilst doubling and halving the total soluble mass to 5.4 and 1.35ng respectively (referred to as tests T_double_mass and T_half_mass). These tests were designed to investigate the sensitivity of the fog development and structure to both CCN number and size.

CCN number concentration

As shown in Figure 3, the mean visibility for T_double_ccn is lower than T_control throughout the simulation by up to a factor of 0.52, with the formation of fog occurring at 1700 UTC (the beginning of the simulation) and the simulation eventually converging to a visibility of around 96m. As with T_control, the spatial variation between the minimum and maximum visibility is not appreciably different prior to 2100 UTC for T_double_ccn. However, after this point the range increases to a maximum of 50m. In comparison with the observations, T_double_ccn's visibility is lower throughout much of the simulation. A decrease in visibility with an increase in CCN number concentration is to be expected, as increasing the CCN number results in a higher number of smaller fog droplets being formed for a given liquid water path, therefore increasing the fog optical depth (Twomey, 1977). A consequence of the increase in optical depth is an enhanced rate of cooling above the fog layer, resulting in the fog layer becoming well mixed too quickly (for this example, the cooling rate increased from 1.7 to 2.41Khr^{-1} at the top of the fog layer between T_control and T_double_ccn).

The simulated mean visibility in T_half_ccn shows the best agreement with the observed visibility in the early stages of fog development (Figure 3). Fog began to form 45min prior to the timings recorded in the observations due to the decrease in CDNC throughout the simulation, as seen in Figure 4 (for this case the CCN ≈ CDNC). The mean visibility within the simulation eventually converges to around 260m (Figure 3) and is greater than T_control by a factor of 1.7. Of all three simulations, T_half_ccn appears to have the most spatial variation, with the most variation occurring from 0000 UTC onwards. In addition, Figure 5 shows a decrease in the LWP as the CCN number concentration decreases (as previously shown in Stolaki *et al.*, 2015). This result is again physically expected, as decreasing the CCN concentration results in an increase in the average drop size and hence an enhanced rate of sedimentation, leading to a reduced longwave cooling rate and thus a decrease in the production rate of liquid water.

So far, the sensitivity studies have shown that increasing CCN results in optically thicker fog; however, it seems that the model is consistently overpredicting aerosol activation and hence CDNC. Such an overprediction may be the result of the underlying design of the aerosol activation scheme. Traditionally, aerosol activation parameterisations are designed using a system that solves a time variation in supersaturation, in combination with Köhler theory (e.g. Twomey, 1959; Abdul-Razzak and Ghan, 2000; Ming *et al.*, 2007; Curry and Khvorostyanov, 2012). Köhler theory states that should the maximum supersaturation within the environment be greater than the critical supersaturation for a given aerosol, the aerosol will become activated (Köhler, 1936). The majority of these schemes assume that the change in supersaturation is driven by adiabatic lifting, which links directly to an updraft velocity found in convective clouds. Furthermore, as discussed in Boutle *et al.* (2018), a minimum updraft velocity of 0.1ms^{-1} is often imposed, equivalent to a cooling rate of 3.51Khr^{-1}, assuming a dry adiabatic lapse rate. The threshold was imposed as these schemes were designed to be implemented into general circulation models (GCMs) to account for cloud top turbulence being poorly resolved for resolutions coarser than 100m (Ghan *et al.*, 1997). Both of these assumptions are unsuitable for the representation of aerosol activation in radiation fog, since updraft velocities at the formation stage are close to zero and the change in saturation is driven by radiative cooling from the ground (Price, 2011). Consequently, this may result in the maximum environmental supersaturation being too high, causing too many aerosols to activate and the fog layer to become optically thick too quickly. These results will motivate future work that could investigate the assumptions associated with aerosol activation parameterisations used within CASIM and their validity for simulations of nocturnal radiation fog.

CCN soluble mass

Increasing the total soluble mass will result in larger CCN, which are more likely to activate according to Köhler theory. The aim of this simulation was to understand how sensitive the fog layer evolution is to a given CCN size. Across all time frames (Table 3), the proportion of activated droplets increases for T_double_mass, therefore accounting for the increase and decrease in the visibility and LWP respectively, as shown in Figure 6. By contrast, the proportion of activated droplets decreases for T_half_mass, therefore accounting for the decrease in visibility and increase in LWP. However, the relative change in visibility and LWP for each respective soluble mass test is much lower than it is for the tests with the equivalent proportion change in CCN number. So, although in this case the change in CCN size, and consequently the change in aerosol-size distribution, influences the evolution of the fog layer, further work should be conducted to understand its full impact.

Summary

The focus of this study was the investigation of the importance of aerosol–fog interactions within a nocturnal radiation fog case (LANFEX IOP1). This was split into two

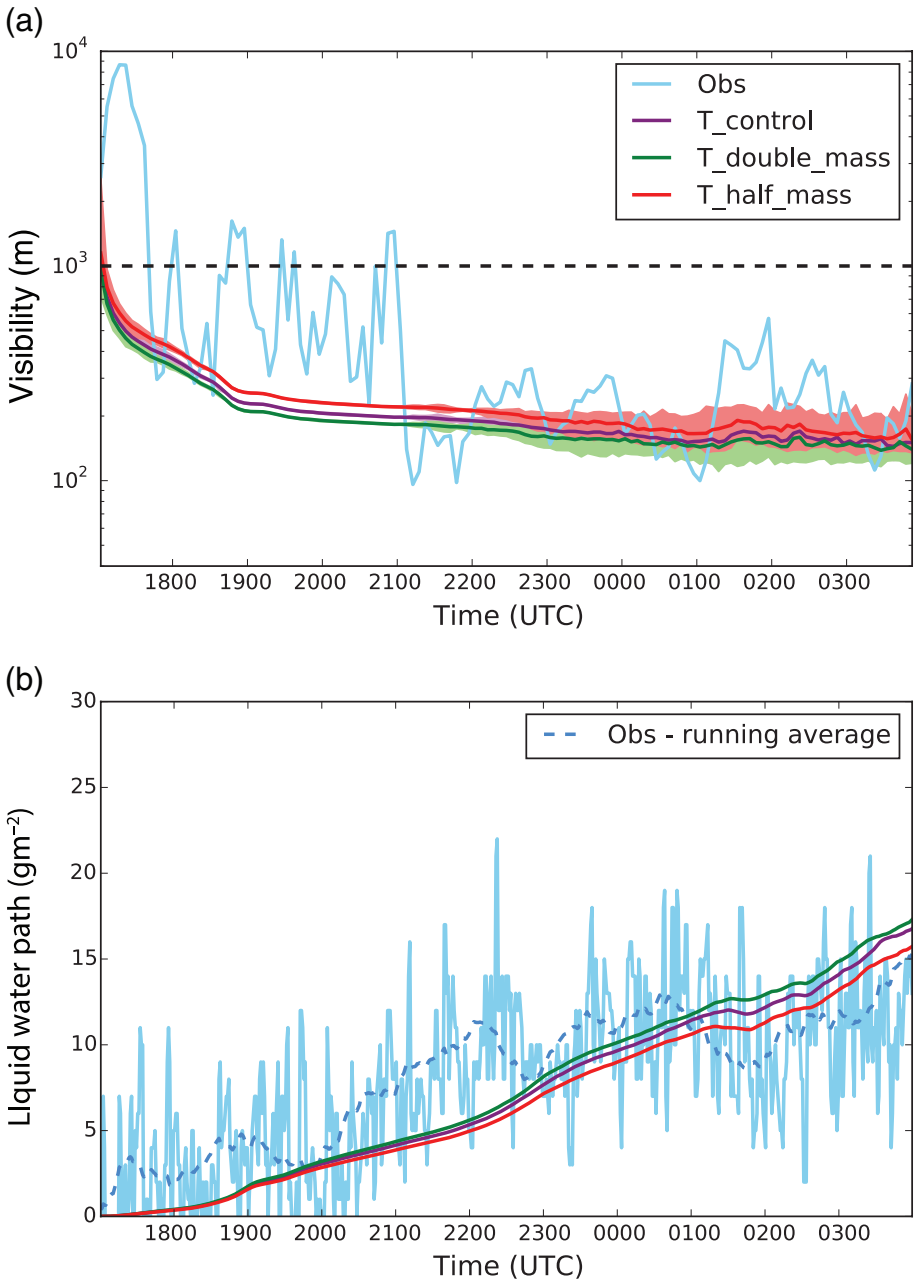

Figure 6. (a) - Time series of mean visibility (m) at 2m height. Purple – T control; green – T_double_mass; red – T_half_mass; light blue – observations. Minimum and maximum visibility mark on figure by shaded area. (b) Time series of liquid water path (gm^{-2}). Purple – T_control; green – T_double_ccn; red – T_half_ccn; sky blue – observations; blue dashed – running average over observations (40 points).

objectives. The first was to evaluate how well MONC coupled with CASIM could simulate IOP1, and identify any potential discrepancies. The conclusion is that although MONC captures the main physical features within IOP1, the fog transitions evolve too fast in comparison to observations, due to the high proportion of modelled to observed fog droplets.

The second objective was to investigate how sensitive the fog evolution is to different aerosol properties. By decreasing the CCN number from 100 to 50cm^{-3}, the simulated rate of transition to optically thick fog is reduced and is more in line with observations from IOP1. Furthermore, the evolution of the fog is sensitive to the change in soluble mass for a given CCN concentration. These results highlight the importance of accurate aerosol initial conditions for simulations of fog. Other aspects such as the aerosol-size distribution may also be important for the evolution of the fog layer (e.g. Zhang *et al.*, 2014). It is planned to investigate this in future work.

The results presented in this study demonstrate the complexity of aerosol–fog interactions and their importance in understanding nocturnal radiation fog. In particular, this study has highlighted why the fog droplet number is important for fog evolution, and why errors in aerosol activation representation may be important. Although previous studies have investigated aerosol–fog interactions, the majority of them simulate cases in highly polluted areas (for example the ParisFog field study by Haeffelin *et al.*, 2010). The main characteristic of the LANFEX dataset, and in particular IOP1, is that it is a 'clean' case with low aerosol concentrations, representing a different regime.

The use of CASIM within MONC has highlighted the importance of including aerosol processes in fog modelling, with the results showing how accounting for different CDNC regimes is needed to represent the transition to optically thick fog. Research is ongoing to develop CASIM, in particular the aerosol activation scheme, and such developments should provide improved capabilities for operational fog forecasting.

Acknowledgements

The authors would like to thank the Met Office Research Unit in Cardington (UK) for providing and processing the observational dataset used throughout this study. C. Poku was supported by a Natural Environment Research Council (NERC) Industrial CASE award with the Met Office (grant number NE/M009955/1). This work used Monsoon2, a collaborative High Performance Computing facility funded by the Met Office and the Natural Environment Research Council. The authors would like to thank the anonymous reviewers for comments that helped improve the quality of this manuscript.

References

Abdul-Razzak H, Ghan SJ. 2000. A parameterization of aerosol activation: 2. Multiple aerosol types. *J. Geophys. Res. Atmos.* **105**(D5): 6837–6844.

BBC. 2013. Sheppey crossing crash: Dozens hurt as 130 vehicles crash. *BBC News.* https://www.bbc.co.uk/news/uk-england-kent-23970047 (accessed 7 February 2019.)

Blyth AM, Latham J. 1991. A climatological parameterization for cumulus clouds. *J. Atmos. Sci.* **48**(21): 2367–2371.

Bott A. 1991. On the influence of the physico-chemical properties of aerosols on the life cycle of radiation fogs. *Boundary Layer Meteorol.* **56**(1–2): 1–31.

Boutle I, Price J, Kudzotsa I *et al.* 2018. Aerosol-fog interaction and the transition to well-mixed radiation fog. *Atmos. Chem. Phys*. **18**: 7827–7840.

Brown N, Weiland M, Hill A *et al.* 2015. A highly scalable Met Office NERC cloud model, in *Proceedings of the 3rd International Conference on Exascale Applications and Software – EASC 2015.* Edinburgh, UK, April 2015. https://dl.acm.org/citation.cfm?id=2820083.2820108 (accessed 29 November 2018.)

Brown N, Weiland M, Hill A *et al.* 2018. In situ data analytics for highly scalable cloud modelling on Cray machines.

Concurr. Comput. Pract. Exp. **30**(1): e4331. doi: 10.1002/cpe.4331.

Curry JA, Khvorostyanov VI. 2012. Assessment of some parameterizations of heterogeneous ice nucleation in cloud and climate models. *Atmos. Chem. Phys.* **12**(2): 1151–1172.

Dearden C, Hill A, Coe H *et al.* 2018. The role of droplet sedimentation in the evolution of low-level clouds over southern West Africa. *Atmos. Chem. Phys.* **18**: 14253–14269.

Edwards JM, Slingo A. 1996. Studies with a flexible new radiation code. I: choosing a configuration for a large-scale model. *Q. J. R. Meteorolog. Soc.* **122**(531): 689–719.

Field P, Shipway B, Hill A *et al.* 2016. *MOSAC and SRG Meetings 2016 – Cloud microphysics and aerosols*. https://www.metoffice.gov.uk/binaries/content/assets/mohippo/pdf/library/mosac/2016/mosac_2016_21.20_fieldetal.pdf (accessed 30 December 2018.)

Ghan SJ, Leung LR, Easter RC *et al.* 1997. Prediction of cloud droplet number in a general circulation model. *J. Geophys. Res. Atmos.* **102**(D18): 21777–21794.

Ghan SJ, Abdul-Razzak H, Nenes A *et al.* 2011. Droplet nucleation: physically-based parameterizations and comparative evaluation. *J. Adv. Model. Earth Syst.* **3**(4).

Gray MEB, Petch J, Derbyshire SH *et al.* 2001. Version 2.3 of the Met. Office large eddy model. Met Office (APR) Turbulence and Diffusion Report 276.

Grosvenor DP, Field PR, Hill AA *et al.* 2017. The relative importance of macrophysical and cloud albedo changes for aerosol-induced radiative effects in closed-cell stratocumulus: insight from the modelling of a case study. *Atmos. Chem. Phys.* **17**(8): 5155–5183.

Gultepe I, Müller MD, Boybeyi Z *et al.* 2006. A new visibility parameterization for warm-fog applications in numerical weather prediction models. *J. Appl. Meteorol. Climatol.* **45**(11): 1469–1480.

Gultepe I, Tardif R, Michaelides SC *et al.* 2007. Fog research: a review of past achievements and future perspectives. *Pure Appl. Geophys.* **164**(6–7): 1121–1159.

Haeffelin M, Bergot T, Elias T *et al.* 2010. PARISFOG: shedding new light on fog physical processes. *Bull. Am. Meteorol. Soc.* **91**(6): 767–783.

Köhler H. 1936. The nucleus in and the growth of hygroscopic droplets. *Trans. Faraday Soc.* **32**: 1152–1161.

Maalick Z, Kühn T, Korhonen H *et al.* 2016. Effect of aerosol concentration and absorbing aerosol on the radiation fog life cycle. *Atmos. Environ.* **133**: 26–33.

Maronga B, Bosveld FC. 2017. Key parameters for the life cycle of nocturnal radiation fog: a comprehensive large-eddy simulation study. *Q. J. R. Meteorolog. Soc.* **143**: 2463–2480

Miltenberger AK, Field PR, Hill AA *et al.* 2018. Aerosol–cloud interactions in mixed-phase convective clouds – Part 1: aerosol perturbations. *Atmos. Chem. Phys.* **18**(5): 3119–3145.

Ming Y, Ramaswamy V, Donner LJ *et al.* 2007. Modeling the interactions between aerosols and liquid water clouds with a self-consistent cloud scheme in a general circulation model. *J. Atmos. Sci.* **64**(4): 1189–1209.

Price J. 2011. Radiation fog. Part I: observations of stability and drop size distributions. *Boundary Layer Meteorol.* **139**(2): 167–191.

Price JD, Lane S, Boutle IA *et al.* 2018. LANFEX: a field and modeling study to improve our understanding and forecasting of radiation fog. *Bull. Am. Meteorol. Soc.* **99**: 2061–2077.

Pruppacher HR, Klett JD. 2010. *Microphysics of Clouds and Precipitation*. Springer: Dordrecht, the Netherlands.

Roach WT, Brown R, Caughey SJ *et al.* 1976. The physics of radiation fog: I -a field study. *Q. J. R. Meteorolog. Soc.* **102**(432): 313–333.

Smith DKE, Renfrew IA, Price JD *et al.* 2018. Numerical modelling of the evolution of the boundary layer during a radiation fog event. *Weather*. **73**(10): 310–316.

Stevens RG, Loewe K, Dearden C *et al.* 2018. A model intercomparison of CCN-limited tenuous clouds in the high Arctic. *Atmos. Chem. Phys.* **18**(15): 11041–11071.

Stolaki S, Haeffelin M, Lac C *et al.* 2015. Influence of aerosols on the life cycle of a radiation fog event. A numerical and observational study. *Atmos. Res.* **151**: 146–161.

Tardif R, Rasmussen RM, Tardif R *et al.* 2007. Event-based climatology and typology of fog in the New York City region. *J. Appl. Meteorol. Climatol.* **46**(8): 1141–1168.

Taylor GI. 1917. The formation of fog and mist. *Q. J. R. Meteorolog. Soc.* **43**(183): 241–268.

Twomey S. 1959. The nuclei of natural cloud formation part II: the supersaturation in natural clouds and the variation of cloud droplet concentration. *Pure Appl. Geophys.* **43**(1): 243–249.

Twomey S. 1977. The Influence of Pollution on the Shortwave Albedo of Clouds. *J. Atmos. Sci.* **34**(7): 1149–1152.

Zhang X, Musson-Genon L, Dupont E *et al.* 2014. On the influence of a simple microphysics parametrization on radiation fog modelling: a case study during ParisFog. *Boundary Layer Meteorol.* **151**(2): 293–315.

Correspondence to: C. Poku

eecp@leeds.ac.uk

doi:10.1002/wea.3503